

# D<sub>2</sub>O: Dynamic Discriminative Operations for Efficient Generative Inference of Large Language Models

Zhongwei Wan<sup>1†\*</sup> Xinjian Wu<sup>2\*</sup> Yu Zhang<sup>3</sup> Yi Xin<sup>4</sup> Chaofan Tao<sup>5</sup> Zhihong Zhu<sup>6</sup>  
Xin Wang<sup>1</sup> Siqu Luo<sup>4</sup> Jing Xiong<sup>5</sup> Mi Zhang<sup>1</sup>

<sup>1</sup>The Ohio State University <sup>2</sup>University of Chinese Academy of Sciences  
<sup>3</sup>Tongji University <sup>4</sup>Nanjing University <sup>5</sup>The University of Hong Kong <sup>6</sup>Peking University  
Correspondence to {wan.512, mizhang.1}@osu.edu

## Abstract

Efficient inference in Large Language Models (LLMs) is impeded by the growing memory demands of key-value (KV) caching, especially for longer sequences. Traditional KV cache eviction strategies, which prioritize less critical KV-pairs based on attention scores, often degrade generation quality, leading to issues such as context loss or hallucinations. To address this, we introduce **Dynamic Discriminative Operations (D<sub>2</sub>O)**, a novel method that utilizes two-level discriminative strategies to optimize KV cache size without fine-tuning, while preserving essential context. Initially, by observing varying densities of attention weights between shallow and deep layers, we use this insight to determine which layers should avoid excessive eviction to minimize information loss. Subsequently, for the eviction strategy in each layer, D<sub>2</sub>O innovatively incorporates a compensation mechanism that maintains a similarity threshold to re-discriminate the importance of previously discarded tokens, determining whether they should be recalled and merged with similar tokens. Our approach not only achieves significant memory savings and enhances inference throughput by more than 3× but also maintains high-quality long-text generation. Extensive experiments across various benchmarks and LLM architectures have demonstrated that D<sub>2</sub>O significantly enhances performance with a constrained KV cache budget.

## 1 Introduction

Large Language Models (LLMs) [1–6] excel in tasks requiring long contexts such as dialog systems [7], document summarization [8], question answering [9], and code completion [10]. Models like LLaMA-3 [3], GPT-4 [1], and Gemini-Pro-1.5 [11] have pushed the boundaries to handle contexts from 8k to 1 million tokens. Such long contexts demand a significant amount of KV cache. For instance, a model with 30 billion parameters, processing inputs of 1024 tokens at a batch size of 128, requires up to 180 GB for KV cache [12]. Such bottleneck underscores the critical need for KV cache optimization to balance memory efficiency and accuracy.

To minimize memory demands of KV cache, one of the most effective methods that achieve promising performance is KV cache eviction, where the key is to precisely identify a subset of KVs to be evicted from the cache. However, existing studies all suffer from both layer-level and token-level information loss. At the **layer level**, existing methods [13, 12, 14–16] equally treat all the layers and indiscriminately evicts KV pairs at each layer. However, not all the layers exhibit the same patterns. Figure 1 visualizes the attention weights on the GSM8K dataset [17]. The shallower layers (layers 0 and 1) display densely interconnected attention maps, while the deeper layers (layers 30 and 31) exhibit a staircase sparse pattern, where attention is localized to specific context

<sup>†</sup> Project leader.

\* Equal contribution.

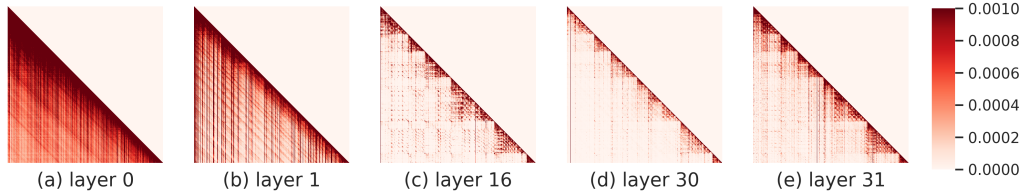


Figure 1: Attention map density comparisons of selected shallow (layers 0, 1) and deep layers (layers 16, 30, 31) of LLaMA-2-7B on the GSM8K dataset. We use the mean value of heads for each layer.

segments, with only a few tokens in each segment receiving substantial attention. This observation aligns with findings from [18, 19], indicating that while shallower layers primarily engage with syntactic structures through global attention, deeper layers target task-related semantic knowledge with localized attention. Consequently, applying the same eviction strategy indiscriminately across all the layers will compromise important information in long contexts. At the **token level**, as shown in Figure 2 (a), existing methods enable models to operate within a constrained KV cache budget by either directly dropping KV pairs (e.g., StreamingLLM [13]) or selectively removing them based on specific eviction policies, such as using cumulative attention scores (e.g., H<sub>2</sub>O [12]) or mean attention scores (e.g., RoCo [16]). However, the irreversible nature of eviction and the difficulty in accurately predicting which KV pairs are essential for future text generation can lead to information loss, causing hallucinations, contextual inconsistencies [20], and challenges in maintaining long content integrity [17, 21].

In this paper, we introduce **Dynamic Discriminative Operations (D<sub>2</sub>O)**, a KV cache eviction method that tackles the two fundamental issues of existing methods described above. The key idea of D<sub>2</sub>O is to incorporate dynamic discriminative operations at both layer level and token level. Specifically, **at layer level**, based on the findings in Figure 1, unlike existing methods [13, 12, 14–16] that indiscriminately evict KV pairs, D<sub>2</sub>O incorporates a tailored KV cache eviction strategy that varies the eviction ratio for each layer based on the density metric of the attention weights. **At token level**, given the uncertainties about how discarded tokens might affect future outputs, D<sub>2</sub>O introduces an effective compensation mechanism by maintaining an exponential moving average (EMA) threshold that assesses the degree of similarity between previously discarded and retained tokens, allowing D<sub>2</sub>O to dynamically decide whether a currently discarded token should be recalled and merged with a similar token retained in the current KV cache according to the current EMA threshold, as shown in Figure 2 (b). Through these two-level operations, D<sub>2</sub>O maintains the KV cache at a consistent size while being able to preserve valuable information from evicted tokens, enabling LLMs to handle the generation of extended texts with improved memory efficiency and high-throughput inference while minimizing the loss of contextual information.

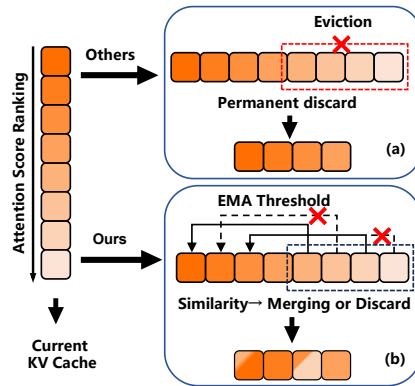


Figure 2: Illustration of D<sub>2</sub>O VS. existing methods. More details are shown in Figure 3.

We compare D<sub>2</sub>O with state-of-the-art KV cache eviction methods StreamingLLM [13], H<sub>2</sub>O [12], and RoCo [16]. To demonstrate the generability of D<sub>2</sub>O, we conduct our evaluation on four models from three different LLM families (Llama, Falcon, and Mistral) and a range of tasks involving math and commonsense reasoning, long-context QA, summarization, and code completion, drawn from LM-Eval [22], LongBench [23], long-context fact retrieval [24], and language modeling [25] benchmarks. We highlight five of our findings: **(1)** D<sub>2</sub>O significantly enhances performance on reasoning tasks, especially with reduced budgets compared to baselines. **(2)** D<sub>2</sub>O manages KV cache compression effectively with minimal accuracy impact, outperforming other eviction-based baselines on LongBench. **(3)** D<sub>2</sub>O demonstrates superior long-context retrieval capabilities with a compressed KV cache compared to baselines. **(4)** D<sub>2</sub>O effectively leverages long-distance dependencies in language modeling with a limited KV cache. **(5)** D<sub>2</sub>O reduces memory usage, enabling up to larger batch sizes and 3 times higher throughput than the full cache setting in our experimental setting.

## 2 Related Work

**KV Cache Eviction.** KV Cache eviction efficiently compresses KV caches by retaining key KVs and discarding less crucial ones. Mistral-7B [4] and Streaming LLM [26] focus on tokens crucial for near-sequence generation. H<sub>2</sub>O [12], Scissorhands [15], and RoCo [16] maintain a small set of influential tokens based on attention scores to enhance generation quality. FlexGen [14] adapts importance policies based on attention scores for KV eviction, while SnapKV [27] uses a recent window strategy to compress KV cache for long prompts, though not specifically for long text generation. However, these methods can significantly lose context from evicted KVs.

**KV Cache Quantization.** Quantization methods aim to compress the bit width of KV cache activations, as seen in several approaches [28–30, 20, 31]. KIVI [30] quantizes the key cache per channel and the value cache per token to reduce the memory requirement. KVQuant [28] integrates multiple technologies, including per-channel key quantization and non-uniform quantization, to quantify the KV cache. Gear [31] combines quantization with low-rank decomposition techniques to reduce cache memory. Additionally, MiKV [20] introduces a mixed-precision approach that maintains less important KV pairs at a lower precision. Our D<sub>2</sub>O model compresses the KV cache into a fixed window size to handle longer texts and preserve context information, providing an orthogonal yet compatible approach with existing methods.

**KV Cache Trainable Compression.** Some methods attempt to adapt LLMs to learn KV cache compression by training on select datasets. LESS [32] learns the residuals between the original and approximated attention outputs from a sparse policy applied during training. DMC [33] pre-trains on original data to learn parameters that control compression across various heads and layers in the KV cache. However, training on partial datasets poses challenges in adapting these methods to diverse downstream tasks due to limited generalizability. Unlike these approaches, our D<sub>2</sub>O employs a plug-and-play method that requires no additional training, offering broader applicability without the need for dataset-specific tuning.

**Token Merging.** Unlike token pruning in encoder-based backbones like ViT [34], which discards less significant tokens, token merging [35, 36] consolidates tokens into fewer, more meaningful units, preserving information integrity. Consequently, token merging has become preferred over token pruning for reducing token count. Existing methods like ToMe [35], TPS [37], MG-ViT [38], and PPT [39] have explored token merging and pruning techniques, primarily in computer vision tasks. In contrast, D<sub>2</sub>O is a pioneering effort to adapt token merging within the KV-Cache, enhancing efficiency for autoregressive tasks in LLMs.

## 3 Preliminary: Generative Inference with KV Cache

A standard generative inference of LLMs includes prompt encoding and token generation.

**Prompt Encoding.** In the prompt encoding stage, a prompt sequence is utilized to generate a KV cache for each transformer layer within LLMs. Consider an input prompt tensor  $\mathbf{X} \in \mathbb{R}^{L_{\text{prompt}} \times D}$ , where  $L_{\text{prompt}}$  represents the length of the prompt and  $D$  denotes the hidden dimension of the model. For simplicity, the indices for heads and layers have been omitted. The key and value tensors are derived as follows:

$$\mathbf{K} = \mathbf{X}\mathbf{W}_K, \mathbf{V} = \mathbf{X}\mathbf{W}_V, \quad (1)$$

With  $\mathbf{W}_K, \mathbf{W}_V \in \mathbb{R}^{D \times D}$  representing the weights for the key and value layers, respectively. Once  $\mathbf{K}$  and  $\mathbf{V}$  are computed, they are stored in the KV cache to facilitate the token generation process [40, 41].

**Token Generation.** In the Token Generation phase, the KV cache is both utilized and updated to sequentially produce tokens. For each time step  $i$ , only the keys and values for the new token  $\mathbf{x}_i$  are computed whereas those for  $\mathbf{x}_{<i}$  are retrieved from the cache. We define the concatenation as  $[\cdot]$ . Then the cache is updated and the output of newly generated token is as:

$$\mathbf{K} = [\mathbf{K}, \mathbf{x}_i\mathbf{W}_K], \mathbf{V} = [\mathbf{V}, \mathbf{x}_i\mathbf{W}_V], \quad (2)$$

$$\mathbf{x}_{i,out} = \text{Softmax}\left(\mathbf{q}_i\mathbf{K}^\top/\sqrt{D}\right)\mathbf{V}, \mathbf{q}_i = \mathbf{x}_i\mathbf{W}_Q, \quad (3)$$

where  $\mathbf{W}_Q \in \mathbb{R}^{D \times D}$  is the weight matrix of the query layer, the linear expansion of the KV cache with each new token significantly increases memory usage and latency, particularly for longer prompts or during token generation. It underscores the importance of compressing the KV cache.

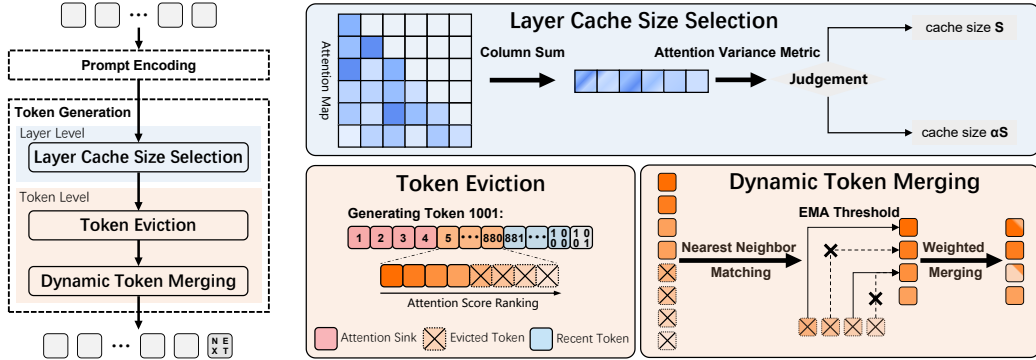


Figure 3: Overview of the proposed D<sub>2</sub>O framework.

## 4 Method

Figure 3 provides an overview of our proposed D<sub>2</sub>O framework. At the layer level, D<sub>2</sub>O addresses the issue of inconsistent attention density across higher and lower layers by incorporating a dynamic cache at each layer (Section 4.1). The size of the cache is determined by the variance metric of attention. At the token level, D<sub>2</sub>O addresses long-context information loss by incorporating a combination of a token eviction scheme and a dynamic token merging technique (Section 4.2).

### 4.1 Layer Level Discriminative Operation

Employing a uniform eviction strategy such as H<sub>2</sub>O [12] or StreamingLLM [13] across all layers could potentially compromise model performance. To address this, we propose using a specific metric,  $F_d$ , to evaluate the attention density of each layer:

$$\mathbf{A}_p = \text{Softmax} \left( \mathbf{Q}_p \mathbf{K}_p^\top / \sqrt{D} \right), \text{ and } F_d = \text{Var} \left( \sum_{i=0}^{L_{\text{prompt}}} \mathbf{A}_p[i, :] \right), \quad (4)$$

where  $\mathbf{A}_p$  denotes the attention score of prompt encoding,  $\mathbf{Q}_p, \mathbf{K}_p \in \mathbb{R}^{L_{\text{prompt}} \times D}$ . We sum the elements of each column in  $\mathbf{A}_p$  to establish the initial state of the cumulative attention sequence. The attention density for each layer is then quantified by the variance of this sequence, with the rationale that denser attention weights correspond to smaller variances. This relationship is illustrated in Figure 4, we observe a consistent phenomenon across all models: the variance of attention scores is lower in the shallow layers (e.g., 0, 1, 2), indicating that the attention weights are dense, as also shown in Figure 1. This density makes it difficult to distinguish which tokens should be discarded. In deeper layers, the variance increases, and the attention weights display a sparse pattern. Based on this consistency, we adjust the KV cache size by setting a gate coefficient  $g$ : layers with a variance higher than  $g$  are allocated a smaller cache size  $S$ , while shallower layers with lower variance are assigned a larger cache size  $\alpha S$ , where  $\alpha$  is a scaling factor relative to  $S$ .

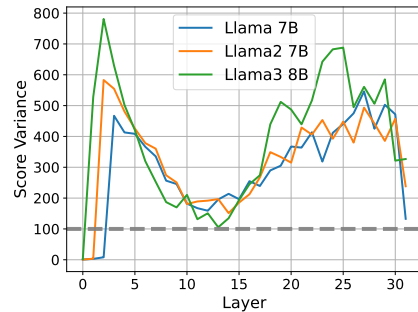


Figure 4: Variances of attention score across different layers for various models.

### 4.2 Token Level Discriminative Operation

After the layer-level discriminative operation, to compensate for the loss of long context information, we introduce two critical steps in the token-level discriminative operation: token eviction and dynamic token merging strategies. Note that our D<sub>2</sub>O is compatible with any token eviction technique. Here, D<sub>2</sub>O primarily utilizes an eviction strategy based on accumulative attention [12] to dynamically prune the KV cache in generation tasks. For token merging, we introduce a new strategy that uses a similarity threshold based on the exponential moving average (EMA) to dynamically determine whether to merge discarded tokens back into the preserved KV cache by weighted merging.

### 4.2.1 Token Eviction

The core concept of token eviction involves dynamically updating the KV cache by leveraging cumulative attention scores. This process systematically excludes the least essential KV pairs to maintain a stable cache size  $S$ , thereby preserving only the most valuable tokens for efficient inference. A recent study [26] suggests that retaining crucial attention sink tokens within the most recent KV cache window enhances the stability of attention score distributions across extended texts. Unlike traditional accumulation-based approaches such as H<sub>2</sub>O [12], our strategy improves performance by maintaining attention sink tokens from the initial  $T$  tokens of the input and integrating them within a recent size window  $M$ . The attention score is formulated as follows:

$$\text{AttnScore} = \begin{cases} \sum_{i=0}^{L_{\text{prompt}}} \mathbf{A}_p[i, :], & \text{if token } i \leq L_{\text{prompt}}, \\ \text{Softmax}(\mathbf{q}_i \mathbf{K}^\top / \sqrt{D}) + \sum_{i=1}^{L_{\text{prompt}}} \mathbf{A}_p[i, :], & \text{otherwise, token generation} \end{cases} \quad (5)$$

After obtaining the current cumulative attention scores, we retain the most recent window consisting of size  $M$  and include  $T$  attention sink tokens. We then select the top  $N$  tokens with the highest scores from the remaining KV cache to complete the eviction. The process is defined as follows:

$$\mathbf{K}_c = [\mathbf{K}[: T, :], \mathbf{K}[I, :], \mathbf{K}[-M :, :]], \quad \mathbf{V}_c = [\mathbf{V}[: T, :], \mathbf{V}[I, :], \mathbf{V}[-M :, :]], \quad (6)$$

$$\text{and } I = \text{Top}_N(\text{AttnScore}[T : -M], N), \quad (7)$$

where  $\text{Top}_N(\cdot, N)$  selects the top  $N$  important tokens with the indices  $I$  in  $\text{AttnScore}$ ,  $(\mathbf{K}_c, \mathbf{V}_c)$  is the conserved KV cache after eviction, and  $S = T + N + M$  denotes the current cache size.

### 4.2.2 Dynamic Token Merging

Then, we obtain the eviction set  $\mathbf{K}_e = \mathbf{K} - \mathbf{K}_c$ . However, directly discarding these tokens will compromise the integrity of the long context. To address this issue, we propose the dynamic token merging approach that retrieves tokens still containing potential value at minimal computational cost and integrates these selected tokens with similar reserved tokens. Considering the alignment properties of KV-pairs, we only compute the similarity matrix on the key’s tokens and share the similarity metric and weighted merging weights with the value’s tokens. We outline this approach in three key steps: nearest-neighbor matching, EMA threshold judgment, and weighted merging.

**Nearest Neighbor Matching.** We implement a many-to-one nearest-neighbor matching algorithm [42] to calculate the similarity matrix  $\mathbf{U}$  between  $\mathbf{K}_e$  and  $\mathbf{K}_c$ . We subsequently identify the most similar tokens from  $\mathbf{K}_c$  as candidates for merging. Specifically, let  $I^e$  and  $I^c$  denote the indices, and  $L^e$  and  $L^c$  represent the lengths of tokens in  $\mathbf{K}_e$  and  $\mathbf{K}_c$ , respectively. Each element  $\mathbf{u}_{i,j}$  in  $\mathbf{U}$  represents the interaction between tokens for matching, where  $i \in I^e$  and  $j \in I^c$ . We then determine the closest token  $\mathbf{k}_*^{\text{nearest}}$  in  $\mathbf{K}_c$  for each evicted token  $\mathbf{k}_i$ . The formulas are as follows:

$$\mathbf{k}_*^{\text{nearest}} = \underset{j \in I^c}{\text{Argmax}}(\mathbf{u}_{i,j}), \text{ where } \mathbf{u}_{i,j} = \frac{\mathbf{k}_i^\top \mathbf{k}_j}{\|\mathbf{k}_i\| \|\mathbf{k}_j\|} \quad (8)$$

Here, we adopt cosine similarity, and  $\|\cdot\|$  is the norm. Given that the similarity matrix  $\mathbf{U} \in \mathbb{R}^{L^e \times L^c}$  is derived directly from input prompts and  $\mathbf{U} \in \mathbb{R}^{L^c}$  during token generation, it introduces no additional parameters and ensures that the computation remains efficient.

**EMA Threshold.** After calculating similarities and identifying candidate tokens  $\{\mathbf{K}_*^{\text{nearest}}\}$ , directly applying average weighted fusion to token pairs can lead to feature dispersion. Additionally, as depicted in Figure 1, attention patterns in higher layers exhibit a staircase-like pattern, indicating a focus on local window information. Besides, since only a few critical tokens exist outside these local windows, indiscriminately merging all candidate tokens can introduce redundant information or noise, ultimately impacting inference accuracy. Inspired by the exponential moving average (EMA) [43, 44] feature used in time-series tasks, which prioritizes more recent data thus enhancing sensitivity to data changes, we propose EMA threshold for token-level operation. Our approach emphasizes the importance of recent similarity between current evicted tokens and conserved tokens while smoothing historical similarity information between previously evicted tokens and conserved tokens. Specifically, the impact of past token similarity thresholds diminishes exponentially over

time, assigning increased weight to more recent thresholds. The EMA threshold is shown as:

$$\tau_t = \begin{cases} \frac{1}{L^e} \sum_{i=0}^{L^e} \text{Max}(\mathbf{U}_t[i, :]), & \text{if } t = 0 \text{ for prompt encoding } \leq L_{\text{prompt}}, \mathbf{U}_t \in \mathbb{R}^{L^e \times L^c} \\ \beta \text{Max}(\mathbf{U}_t[:]) + (1 - \beta) \tau_{t-1} & \text{otherwise, } t > 0 \text{ for token generation, } \mathbf{U}_t \in \mathbb{R}^{L^c} \end{cases} \quad (9)$$

where the initial threshold  $\tau$  is set to the average of the highest similarity values from the eviction token to the conserved set, as calculated within the similarity matrix  $\mathbf{U}_t$  at each forward step  $t$ . The smoothing constant  $\beta$  modulates the balance between the current similarity matrix  $\mathbf{U}_t$  and the previous similarity thresholds  $\tau_{t-1}$ , with higher values of  $\beta$  increasing sensitivity to changes in current similarity. If the maximum similarity of the current evicted token is less than  $\tau_i$ , it is permanently discarded. Otherwise, a weighted merge strategy is used.

**Weighted Merging.** Specifically, for a conserved token, eviction tokens that exhibit higher similarity should be assigned greater weights. Thereby, we use weighted merging instead of averaged merging since the approach mitigates potential errors stemming from imperfect token scoring. The weighted merging formulas are defined as:

$$\mathbf{k}_{cj} = \mathbf{w}_{cj} \mathbf{k}_{cj} + \sum_{\mathbf{k}_{ei} \in \mathbf{K}_e} \mathbf{w}_{ei} \mathbf{k}_{ei}, \quad \mathbf{v}_{cj} = \mathbf{w}_{cj} \mathbf{v}_{cj} + \sum_{\mathbf{v}_{ei} \in \mathbf{V}_e} \mathbf{w}_{ei} \mathbf{v}_{ei}, \quad (10)$$

where  $\mathbf{w}_c$  and  $\mathbf{w}_e$  represent the weights assigned to each reserved and evicted key-value pair, respectively. We adopt a similarity-based weighting strategy, inspired by Graph Attention Network [45]. The weight calculation is as follows:

$$\mathbf{w}_{cj} = \frac{e}{\sum_{\mathbf{k}_{ei} \in \mathbf{K}_e} \exp(\mathbf{u}_{ij}) \mathbf{m}_{ij} + e}, \quad \mathbf{w}_{ei} = \frac{\sum_{\mathbf{k}_{ei} \in \mathbf{K}_e} \exp(\mathbf{u}_{ij}) \mathbf{m}_{ij}}{\sum_{\mathbf{k}_{ei} \in \mathbf{K}_e} \exp(\mathbf{u}_{ij}) \mathbf{m}_{ij} + e}. \quad (11)$$

According to the formulas,  $\mathbf{m}_{i,j} \in \mathbf{M}$  is the mask matrix of  $\mathbf{U}$ . If  $\mathbf{x}_j \in \mathbf{K}_c$  is the most similar token to  $\mathbf{x}_i \in \mathbf{K}_e$ , then  $\mathbf{m}_{i,j} = 1$ ; otherwise,  $\mathbf{m}_{i,j} = 0$ . The fusion weights  $\mathbf{w}_{cj}$  and  $\mathbf{w}_{ei}$  are determined by the mask values  $\mathbf{m}_{i,j}$  and similarities  $\mathbf{u}_{i,j}$ . Specifically,  $\mathbf{w}_{ei}$  represents the weight for each evicted token  $\mathbf{k}_{ei}$ , while  $\mathbf{w}_{cj}$  pertains to the weight of the conserved token itself. Each conserved token  $\mathbf{k}_{cj}$  retains the highest fusion weight, as its self-similarity equals 1. Thereby, conserved tokens are not selected as the most similar tokens remain unchanged, whereas evicted tokens are integrated into the most similar ones, replacing the originals.

## 5 Experiment

### 5.1 Experimental Settings

**Backbones.** We evaluate D<sub>2</sub>O using four models: Llama-2 [2], Llama-3 [3], Falcon [46], and Mistral [4]. For Llama-2, we employ model sizes ranging from 7B to 13B. For Llama-3, we use an 8B model. Notably, both the Llama-2 and Mistral models utilize multi-head attention, while Falcon employs multi-query attention [47] and Llama-3 uses grouped query attention [48]. We implement the D<sub>2</sub>O algorithm using the Hugging Face Transformers codebase [49].

**Tasks.** We evaluate D<sub>2</sub>O using datasets with both standard and extended context lengths. For standard contexts, we utilize generation tasks from LM-Eval [22], assessing model performance across commonsense and math reasoning on CoQA (Exact Match Accuracy)[50], TruthfulQA (BLEU score)[51], and GSM8K (Exact Match Accuracy)[52]. For long-context tasks, we apply LongBench [23], which is particularly suited for evaluating the effects of compressed KV cache. This involves tasks from subgroups such as Single-Document QA, Multi-Document QA, Summarization, Synthetic, and Code Completion. Additionally, we assess D<sub>2</sub>O’s capability in long-context retrieval with the Needle-in-a-Haystack test [53], challenging the model to retrieve a specific sentence within a large document. We also validate our method’s long sequence modeling ability using PG-19 [25]. More details are illustrated in Appendix A.3.

**Implementation.** In our principal experiment, we set the gate coefficient  $g = 100$  for layer-level operations, as determined by the statistics in Figure 4. With the help of grid search, the scaling factor  $\alpha$  was set to  $2 \sim 4$ , and the  $\beta$  for EMA threshold merging was set to  $0.5 \sim 0.9$ . The number of top  $N$  important tokens and the recent token  $M$  are based on the ratio of  $L_{\text{prompt}}$ , typically  $N : M = 3 : 1$ , with  $N + M = rL$ . The parameter  $r$  varied across settings, including values such as 0.2, 0.4, and 0.8. All experiments were conducted on NVIDIA A100 80GB GPUs. Further details on implementation and additional ablations are provided in Section 5.5.

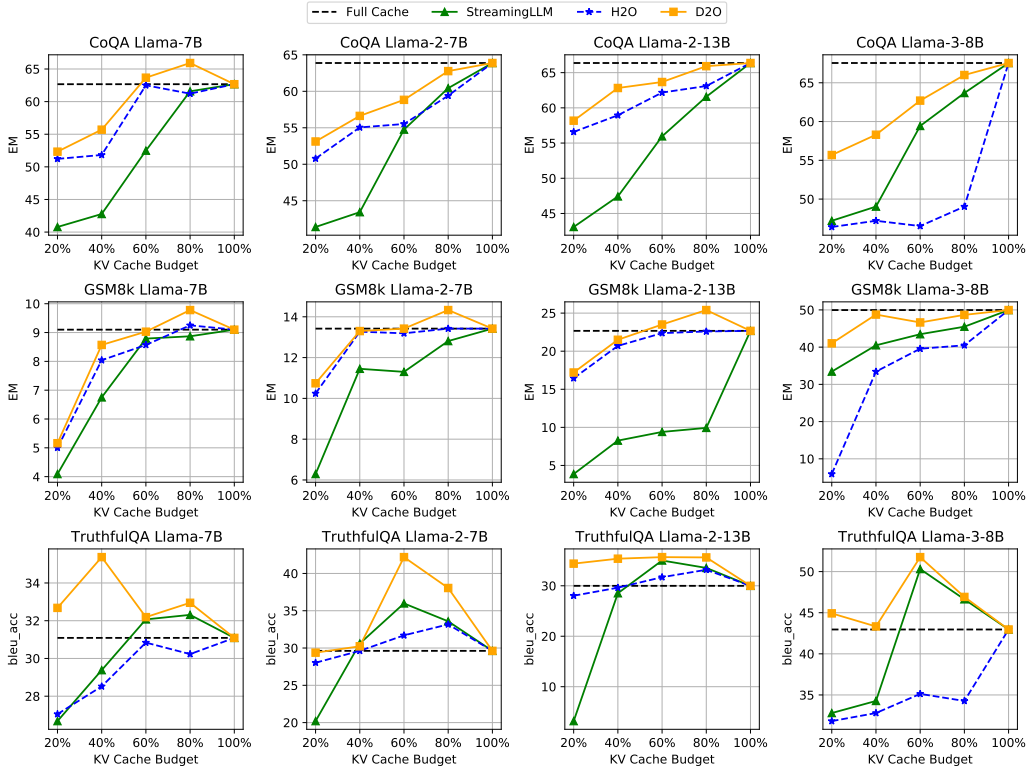


Figure 5: Performance of  $D_2O$  and other methods for Llama backbones on reasoning datasets including CoQA, GSM8k, TruthfulQA.

## 5.2 Comparative Analysis of KV Cache Compression Ratios

In Figure 5, we benchmark  $D_2O$  on GSM8K, CoQA, and TruthfulQA datasets. We compare models equipped with a full KV cache against those utilizing our  $D_2O$  compression technique over several Llama models: Llama-1-7B, Llama-2-7B, Llama-2-13B, and the latest Llama-3-8B. The ratio represents the proportion of the compressed KV cache budget to the prompt length  $L_{\text{prompt}}$ . Results indicate that  $D_2O$  consistently outperforms all other KV compression methods across all configurations. Notably,  $D_2O$  significantly enhances performance, particularly under reduced budgets. This performance reflects the ability of  $D_2O$ 's context retention strategy to compensate for the severe loss of contextual information inherent in eviction-based methods and prevent the degradation of LLMs's reasoning capabilities, particularly for Llama-3-8B on the GSM8K and CoQA datasets. Intriguingly, on the TruthfulQA dataset,  $D_2O$  even outperforms the full model across four Llama backbone settings and most of the budget ratios, demonstrating that  $D_2O$ 's unified eviction and dynamic merging strategies can prune irrelevant tokens from LLMs' input texts, preserving essential context and then enhancing reasoning accuracy.

## 5.3 Accuracy Comparison on Long-context Tasks

**LongBench Results.** We evaluate  $D_2O$  on five models using LongBench, as shown in Table 1, including Falcon-7B, Mistral-7B, Llama-2-7B, Llama-2-13B, and Llama-3-8B. To assess the performance of  $D_2O$  and various baselines under high compression conditions, we set the default KV cache budget ratio at 20%. Table 1 demonstrates that  $D_2O$  effectively manages KV cache compression with minimal impact on accuracy, and successfully captures key information in lengthy texts compared to the full model. Notably, the local window method exhibits severe performance degradation due to significant context loss. Furthermore, we compare  $D_2O$  with other recent eviction-based baselines to further demonstrate  $D_2O$ 's capability to retain key information. The results show that  $D_2O$  significantly outperforms other eviction-based methods, such as StreamingLLM [26], H<sub>2</sub>O [12], and RoCo [16], especially on the Llama-3-8B backbone.

Table 1: Performance evaluation of D<sub>2</sub>O on various models in LongBench benchmarks. For each baseline, except for the full model, we retain 20% of  $L_{\text{prompt}}$  as the preserved KV cache size and highlight the best method.

Methods	Single-Document QA			Multi-Document QA			Summarization			Summarization			Synthetic		Code		
	NrivQA	Qasper	MF-en	HopqaQA	2WikiMQA	Musique	GovReport	QMSum	MultiNews	TREC	TriviaQA	SAMSum	PCount	Pre	Lcc	RB-P	
<b>Falcon-7B</b>	Full Model	1.03	3.82	7.62	1.75	1.78	1.25	3.77	2.48	6.04	5.00	8.27	2.73	0.49	0.41	9.98	7.33
	Local Window	0.43	2.60	4.80	1.26	1.31	0.50	1.79	0.61	2.31	4.67	7.00	1.72	0.84	0.39	8.95	<b>7.28</b>
	StreamingLLM	0.32	2.61	4.85	1.56	1.04	<b>0.54</b>	1.80	0.53	4.54	4.67	6.53	1.68	1.60	0.36	9.67	7.16
	H <sub>2</sub> O	0.43	4.01	5.65	1.66	1.70	0.50	2.61	0.61	4.36	4.33	7.57	2.20	0.53	0.0	10.57	6.72
	RoCo	0.38	3.82	5.33	1.31	1.61	0.38	2.25	0.53	3.88	4.35	7.42	1.88	0.49	0.22	9.78	6.75
	D <sub>2</sub> O	<b>0.87</b>	<b>4.20</b>	<b>6.49</b>	<b>1.68</b>	<b>1.76</b>	0.43	<b>2.80</b>	<b>2.79</b>	<b>4.60</b>	<b>4.93</b>	<b>8.34</b>	<b>2.29</b>	<b>1.61</b>	<b>0.55</b>	<b>10.77</b>	7.08
<b>Mistral-7B</b>	Full Model	26.28	29.8	49.44	41.77	26.52	19.35	33.32	24.44	26.28	66.67	86.16	41.11	4.43	90.5	56.91	49.09
	Local Window	16.25	15.72	29.25	27.88	19.55	12.80	21.64	15.71	15.45	33.65	26.54	18.57	2.35	41.25	28.50	26.50
	StreamingLLM	18.75	16.22	33.54	29.77	19.42	13.34	18.55	17.78	17.54	50.52	62.76	20.88	2.39	45.22	52.31	33.28
	H <sub>2</sub> O	22.45	23.52	42.78	33.56	23.45	15.58	28.48	18.88	20.22	56.72	75.52	32.88	3.45	78.55	52.38	37.25
	RoCo	19.55	21.22	38.54	29.88	19.98	13.38	25.22	15.32	16.85	52.45	76.23	30.50	2.88	75.58	49.54	38.75
	D <sub>2</sub> O	<b>23.55</b>	<b>24.88</b>	<b>44.56</b>	<b>33.89</b>	<b>24.12</b>	<b>16.53</b>	<b>28.89</b>	<b>21.28</b>	<b>23.23</b>	<b>62.13</b>	<b>83.21</b>	<b>37.52</b>	<b>3.55</b>	<b>85.74</b>	<b>54.33</b>	<b>45.25</b>
<b>Llama-2-7B</b>	Full Model	15.02	8.92	21.89	9.12	10.2	3.71	19.45	21.29	1.42	61.00	89.81	39.73	2.49	4.94	67.95	55.14
	Local Window	3.27	6.56	2.3	8.88	7.29	1.25	0.06	2.07	0.28	17.67	4.55	4.70	1.44	5.88	17.69	13.81
	StreamingLLM	10.31	5.62	19.75	6.65	8.75	2.49	1.29	19.86	<b>1.32</b>	52.67	88.96	37.13	0.59	6.10	64.76	50.49
	H <sub>2</sub> O	14.31	7.15	<b>20.45</b>	8.61	9.93	3.29	9.96	20.22	0.40	59.67	88.46	39.61	2.31	<b>7.75</b>	65.00	53.40
	RoCo	12.22	6.58	18.45	7.76	7.95	3.52	8.88	19.56	0.55	57.65	85.54	36.14	2.55	4.84	61.59	50.55
	D <sub>2</sub> O	<b>16.35</b>	<b>7.48</b>	19.91	<b>8.97</b>	<b>10.40</b>	<b>3.93</b>	<b>15.71</b>	<b>21.22</b>	1.08	<b>59.71</b>	<b>89.68</b>	<b>39.96</b>	<b>3.37</b>	6.79	<b>66.45</b>	<b>53.47</b>
<b>Llama-2-13B</b>	Full Model	12.91	9.37	19.65	11.19	10.84	5.59	19.39	21.37	4.74	63.33	87.37	42.3	4.67	7.92	67.36	54.62
	Local Window	3.77	5.17	2.78	13.83	11.76	3.98	0.14	1.48	0.32	17.67	7.54	3.63	0.67	3.89	18.44	13.64
	StreamingLLM	7.19	5.70	11.62	<b>14.06</b>	10.20	4.51	2.28	17.91	0.39	52.00	85.25	37.64	2.17	5.00	64.05	46.34
	H <sub>2</sub> O	13.52	6.53	15.10	10.74	10.74	5.28	12.13	20.48	0.29	60.33	85.73	42.23	3.25	9.52	64.98	51.31
	RoCo	11.01	4.88	14.05	10.22	9.78	4.95	9.54	19.85	1.07	55.56	84.78	38.95	3.22	6.02	63.21	51.95
	D <sub>2</sub> O	<b>13.69</b>	<b>7.35</b>	<b>16.21</b>	10.34	<b>11.88</b>	<b>5.42</b>	<b>15.68</b>	<b>20.75</b>	<b>2.66</b>	<b>61.67</b>	<b>87.69</b>	<b>42.48</b>	<b>5.33</b>	<b>9.33</b>	<b>66.25</b>	<b>52.14</b>
<b>Llama-3-8B</b>	Full Model	14.25	12.89	22.45	11.03	12.17	6.98	30.80	23.25	4.02	71.00	90.10	42.08	6.33	12.51	72.94	61.26
	Local Window	1.78	4.64	4.10	6.11	6.91	2.81	0.56	10.33	0.02	33.5	28.67	10.56	5.69	2.00	32.80	23.68
	StreamingLLM	10.47	9.96	13.82	9.64	11.05	5.53	19.99	20.53	3.13	62.67	90.05	41.30	5.44	14.05	70.44	57.93
	H <sub>2</sub> O	13.27	11.05	17.72	10.38	11.23	6.38	21.29	21.33	3.38	66.63	89.19	41.12	5.52	11.11	71.86	58.29
	RoCo	10.77	10.55	16.54	9.98	8.95	9.52	20.78	20.15	2.59	63.98	86.26	38.59	5.55	10.05	68.78	56.66
	D <sub>2</sub> O	<b>13.76</b>	<b>12.04</b>	<b>19.65</b>	<b>11.27</b>	<b>12.26</b>	<b>6.73</b>	<b>24.05</b>	<b>23.09</b>	<b>3.40</b>	<b>69.00</b>	<b>90.33</b>	<b>42.09</b>	<b>6.11</b>	<b>14.12</b>	<b>72.02</b>	<b>59.29</b>

**Long Context Fact Retrieval Task.** To validate D<sub>2</sub>O’s retrieval capabilities in long contexts after compressing the KV cache, we employ the ‘Needle In A Haystack’ task [24], designed to retrieve specific ‘needles’ from extensive documents. We adopted the evaluation settings from the Retrieval Head study, using Llama-2-7B-80k as the backbone of the experiment. For a fair comparison, the KV cache budget was set to 4096, and both D<sub>2</sub>O and baseline models were tested on contexts with maximum lengths of 50k and 100k. The average accuracy is reported in Table 2. D<sub>2</sub>O not only outperforms other eviction-based methods but also exhibits the smallest accuracy drop when compared to the full model. These results underscore D<sub>2</sub>O’s robust long-context retrieval capabilities even with a compressed KV cache.

Table 2: Needle-in-a-haystack results.

Methods	L=50k	L=100k
Full Model	97.88	94.46
StreamingLLM [13]	58.64	47.93
H <sub>2</sub> O [12]	79.84	69.81
SnapKV [27]	83.55	76.22
D <sub>2</sub> O	88.67	83.98

**Long Sequence Modeling Perplexity.** We sample data from the PG-19 [25] and to evaluate the long language modelling perplexity of D<sub>2</sub>O. To ensure a fair comparison, we set the capacity of the KV cache to 2048. Figure 6 depicts the cumulative average negative log-likelihood (NLL) as a function of context length. D<sub>2</sub>O enables LLMs to handle long sequences and achieve superior performance (lower perplexity) compared to other eviction-based compression methods. The results demonstrate that D<sub>2</sub>O can effectively leverage long-distance dependencies in language modeling with a limited KV cache budget.

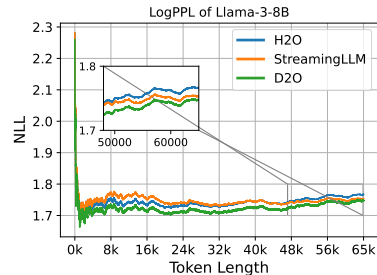


Figure 6: Long sequence modeling PPL.

## 5.4 Throughput Analysis

We demonstrate that reducing the KV cache with D<sub>2</sub>O significantly enhances real-world throughput, as illustrated in Table 3. All experiments are conducted using the Llama-3-8B architecture on an A100-80G GPU without CPU offloading. The KV cache budget is set to be the same as the length of



the prompts to maintain the contextual integrity of the input prompts. We observe that D<sub>2</sub>O reduces memory usage, enabling larger batch sizes and higher throughput. Specifically, as text length increases, D<sub>2</sub>O’s throughput advantage over the entire model also grows. For example, throughput improves from 2.3× at the 256+1024 setting to 3.0× at the 2048+8192 setting, showing D<sub>2</sub>O’s efficiency in processing longer texts.

Table 3: Throughput comparison of full model and D<sub>2</sub>O. 32 (256) means the max batch size is 32 with a 256 cache budget.

Prompt+Gen	256+1024	512+2048	1024+4096	2048+8192
<b>Max Batch Size</b>				
Full Model	8	4	2	1
D <sub>2</sub> O	32 (256)	16 (512)	8 (1024)	4 (2048)
<b>Throughput: tokens/s</b>				
Full Model	374.79	198.94	96.95	43.44
D <sub>2</sub> O	863.62 (2.3×)	479.50 (2.41×)	267.28 (2.75×)	130.45 (3.00×)

## 5.5 Ablation Study

In this section, we conduct a series of experiments on CoQA and trec to investigate the importance of each component and parameter setting in our proposed method. Unless otherwise specified, the Llama-3-8B is used as the default model under 20% cache budget.

**Effectiveness of Layer Discriminative Operation.** To evaluate the effectiveness of the layer-level discriminative operation in our proposed method. We compare the performance of our D<sub>2</sub>O with and without using this strategy. As shown in Table 4, using our layer-level strategy improves the performance on both the reasoning task and summarization task, demonstrating its effectiveness.

Table 4: Performance comparison *w.* or *w/o.* token selection.

Methods	CoQA	TREC
<i>w/o.</i> layer operation	55.9	66.8
<i>w.</i> layer operation	<b>58.2</b>	<b>69.0</b>

**Token Similarity Metric.** Here we discuss various choices based on keys, values, or both of them for token similarity metrics to determine which tokens should be merged. As shown in Table 5, the attention keys ( $\mathcal{K}$ ) exhibit significantly higher performance than the attention values ( $\mathcal{V}$ ). Additionally, we observe a notable decrease in performance when using independent metrics for the key-value ( $\mathcal{K}/\mathcal{V}$ ) cache, which we attribute to the disruption of the corresponding relationships between key-value pairs within the cache.

Table 5: Feature choice.

feature	CoQA	TREC
$\mathcal{K}$	<b>58.2</b>	<b>69.0</b>
$\mathcal{V}$	54.7	64.3
$\mathcal{K}/\mathcal{V}$	53.6	62.7

**Merge Policy.** After deciding what tokens to merge, we explore the policy for token merging in our proposed method. Specifically, we compare the performance of average merging and weighted merging. The results reported in Table 6 reflect that the weighted average policy could achieve better performance.

Table 6: Performance comparison with different merge policy.

Methods	CoQA	TREC
Average	56.2	67.3
Weighted average	<b>58.2</b>	<b>69.0</b>

**Balancing Important Token Size ( $N$ ) and Recent Size ( $M$ ).** We also investigate the impact of different important token sizes and recent size ratios on performance, given a fixed budget. This ratio determines the emphasis placed on influential tokens from a historical context (larger ratio) versus tokens from a recent context (smaller ratio). The results in Table 7 suggest that important tokens reflecting global information seem to have a larger impact on performance.

Table 7: Ratio impact

Methods	CoQA	TREC
1:1	56.5	67.4
1:3	55.4	65.8
3:1	<b>58.2</b>	<b>69.0</b>

## 6 Conclusion

In this paper, we propose Dynamic Discriminative Operations (D<sub>2</sub>O) that can effectively address the challenges of KV cache management in LLMs by dynamically merging tokens to maintain essential contextual information without requiring fine-tuning. By leveraging the varying densities of attention features across layers, D<sub>2</sub>O minimizes information loss during eviction and significantly reduces both computational and memory demands. Our experiments confirm that D<sub>2</sub>O not only preserves the quality of generation in long-text scenarios but also achieves an optimal balance between KV-cache compression and performance. Future research could explore integrating D<sub>2</sub>O with additional compression methods like quantization, distillation, and efficient attention architectures.

## References

- [1] Josh Achiam, Steven Adler, Sandhini Agarwal, Lama Ahmad, Ilge Akkaya, Florencia Leoni Aleman, Diogo Almeida, Janko Altenschmidt, Sam Altman, Shyamal Anadkat, et al. Gpt-4 technical report. *arXiv preprint arXiv:2303.08774*, 2023.
- [2] Hugo Touvron, Louis Martin, Kevin Stone, Peter Albert, Amjad Almahairi, Yasmine Babaei, Nikolay Bashlykov, Soumya Batra, Prajjwal Bhargava, Shruti Bhosale, et al. Llama 2: Open foundation and fine-tuned chat models. *arXiv preprint arXiv:2307.09288*, 2023.
- [3] Meta. Introducing meta llama 3: The most capable openly available llm to date, 2024. URL <https://ai.meta.com/blog/meta-llama-3/>.
- [4] Albert Q Jiang, Alexandre Sablayrolles, Arthur Mensch, Chris Bamford, Devendra Singh Chaplot, Diego de las Casas, Florian Bressand, Gianna Lengyel, Guillaume Lample, Lucile Saulnier, et al. Mistral 7b. *arXiv preprint arXiv:2310.06825*, 2023.
- [5] Zhongwei Wan, Xin Wang, Che Liu, Samiul Alam, Yu Zheng, Zhongnan Qu, Shen Yan, Yi Zhu, Quanlu Zhang, Mosharaf Chowdhury, et al. Efficient large language models: A survey. *arXiv preprint arXiv:2312.03863*, 1, 2023.
- [6] Xin Wang, Zhongwei Wan, Arvin Hekmati, Mingyu Zong, Samiul Alam, Mi Zhang, and Bhaskar Krishnamachari. Iot in the era of generative ai: Vision and challenges. *arXiv preprint arXiv:2401.01923*, 2024.
- [7] Wei-Lin Chiang, Zhuohan Li, Zi Lin, Ying Sheng, Zhanghao Wu, Hao Zhang, Lianmin Zheng, Siyuan Zhuang, Yonghao Zhuang, Joseph E Gonzalez, et al. Vicuna: An open-source chatbot impressing gpt-4 with 90%\* chatgpt quality, march 2023. URL <https://lmsys.org/blog/2023-03-30-vicuna>, 3(5), 2023.
- [8] Tianyi Zhang, Faisal Ladhak, Esin Durmus, Percy Liang, Kathleen R. McKeown, and Tatsunori B. Hashimoto. Benchmarking large language models for news summarization. *CoRR*, abs/2301.13848, 2023.
- [9] Ehsan Kamaloo, Nouha Dziri, Charles LA Clarke, and Davood Rafiei. Evaluating open-domain question answering in the era of large language models. *arXiv preprint arXiv:2305.06984*, 2023.
- [10] Baptiste Roziere, Jonas Gehring, Fabian Gloeckle, Sten Sootla, Itai Gat, Xiaoqing Ellen Tan, Yossi Adi, Jingyu Liu, Tal Remez, Jérémy Rapin, et al. Code llama: Open foundation models for code. *arXiv preprint arXiv:2308.12950*, 2023.
- [11] Machel Reid, Nikolay Savinov, Denis Teplyashin, Dmitry Lepikhin, Timothy Lillicrap, Jean-baptiste Alayrac, Radu Soricut, Angeliki Lazaridou, Orhan Firat, Julian Schrittwieser, et al. Gemini 1.5: Unlocking multimodal understanding across millions of tokens of context. *arXiv preprint arXiv:2403.05530*, 2024.
- [12] Zhenyu Zhang, Ying Sheng, Tianyi Zhou, Tianlong Chen, Lianmin Zheng, Ruisi Cai, Zhao Song, Yuandong Tian, Christopher Ré, Clark Barrett, et al. H2o: Heavy-hitter oracle for efficient generative inference of large language models. *Advances in Neural Information Processing Systems*, 36, 2024.
- [13] Guangxuan Xiao, Yuandong Tian, Beidi Chen, Song Han, and Mike Lewis. Efficient streaming language models with attention sinks. *arXiv preprint arXiv:2309.17453*, 2023.
- [14] Suyu Ge, Yunan Zhang, Liyuan Liu, Minjia Zhang, Jiawei Han, and Jianfeng Gao. Model tells you what to discard: Adaptive kv cache compression for llms. *arXiv preprint arXiv:2310.01801*, 2023.
- [15] Zichang Liu, Aditya Desai, Fangshuo Liao, Weitao Wang, Victor Xie, Zhaozhuo Xu, Anastasios Kyrillidis, and Anshumali Shrivastava. Scissorhands: Exploiting the persistence of importance hypothesis for LLM KV cache compression at test time. In *NeurIPS*, 2023.
- [16] Siyu Ren and Kenny Q. Zhu. On the efficacy of eviction policy for key-value constrained generative language model inference. *CoRR*, abs/2402.06262, 2024.

- [17] Karl Cobbe, Vineet Kosaraju, Mohammad Bavarian, Mark Chen, Heewoo Jun, Lukasz Kaiser, Matthias Plappert, Jerry Tworek, Jacob Hilton, Reiichiro Nakano, Christopher Hesse, and John Schulman. Training verifiers to solve math word problems. *CoRR*, abs/2110.14168, 2021.
- [18] Haiyan Zhao, Hanjie Chen, Fan Yang, Ninghao Liu, Huiqi Deng, Hengyi Cai, Shuaiqiang Wang, Dawei Yin, and Mengnan Du. Explainability for large language models: A survey. *ACM Transactions on Intelligent Systems and Technology*, 15(2):1–38, 2024.
- [19] Haiyan Zhao, Fan Yang, Bo Shen, Himabindu Lakkaraju, and Mengnan Du. Towards uncovering how large language model works: An explainability perspective. 2024. URL <https://api.semanticscholar.org/CorpusID:267740636>.
- [20] June Yong Yang, Byeongwook Kim, Jeongin Bae, Beomseok Kwon, Gunho Park, Eunho Yang, Se Jung Kwon, and Dongsoo Lee. No token left behind: Reliable KV cache compression via importance-aware mixed precision quantization. *CoRR*, abs/2402.18096, 2024.
- [21] Ge Bai, Jie Liu, Xingyuan Bu, Yancheng He, Jiaheng Liu, Zhanhui Zhou, Zhuoran Lin, Wenbo Su, Tiezheng Ge, Bo Zheng, and Wanli Ouyang. Mt-bench-101: A fine-grained benchmark for evaluating large language models in multi-turn dialogues. *CoRR*, abs/2402.14762, 2024.
- [22] Leo Gao, Jonathan Tow, Stella Biderman, Sid Black, Anthony DiPofi, Charles Foster, Laurence Golding, Jeffrey Hsu, Kyle McDonell, Niklas Muennighoff, et al. A framework for few-shot language model evaluation. *Version v0. 0.1. Sept*, page 8, 2021.
- [23] Yushi Bai, Xin Lv, Jiajie Zhang, Hongchang Lyu, Jiankai Tang, Zhidian Huang, Zhengxiao Du, Xiao Liu, Aohan Zeng, Lei Hou, et al. Longbench: A bilingual, multitask benchmark for long context understanding. *arXiv preprint arXiv:2308.14508*, 2023.
- [24] G Kamradt. Needle in a haystack–pressure testing llms, 2023.
- [25] Jack W Rae, Anna Potapenko, Siddhant M Jayakumar, and Timothy P Lillicrap. Compressive transformers for long-range sequence modelling. *arXiv preprint arXiv:1911.05507*, 2019.
- [26] Guangxuan Xiao, Yuandong Tian, Beidi Chen, Song Han, and Mike Lewis. Efficient streaming language models with attention sinks. *CoRR*, abs/2309.17453, 2023.
- [27] Yuhong Li, Yingbing Huang, Bowen Yang, Bharat Venkitesh, Acyr F. Locatelli, Hanchen Ye, Tianle Cai, Patrick Lewis, and Deming Chen. Snapkv: Llm knows what you are looking for before generation. 2024. URL <https://api.semanticscholar.org/CorpusID:269303164>.
- [28] Coleman Hooper, Sehoon Kim, Hiva Mohammadzadeh, Michael W Mahoney, Yakun Sophia Shao, Kurt Keutzer, and Amir Gholami. Kvquant: Towards 10 million context length llm inference with kv cache quantization. *arXiv preprint arXiv:2401.18079*, 2024.
- [29] Yuxuan Yue, Zhihang Yuan, Haojie Duanmu, Sifan Zhou, Jianlong Wu, and Liqiang Nie. Wkvquant: Quantizing weight and key/value cache for large language models gains more. *arXiv preprint arXiv:2402.12065*, 2024.
- [30] Zirui Liu, Jiayi Yuan, Hongye Jin, Shaochen Zhong, Zhaozhuo Xu, Vladimir Braverman, Beidi Chen, and Xia Hu. Kivi: A tuning-free asymmetric 2bit quantization for kv cache. *arXiv preprint arXiv:2402.02750*, 2024.
- [31] Hao Kang, Qingru Zhang, Souvik Kundu, Geonhwa Jeong, Zaoxing Liu, Tushar Krishna, and Tuo Zhao. Gear: An efficient kv cache compression recipe for near-lossless generative inference of llm. *arXiv preprint arXiv:2403.05527*, 2024.
- [32] Harry Dong, Xinyu Yang, Zhenyu Zhang, Zhangyang Wang, Yuejie Chi, and Beidi Chen. Get more with less: Synthesizing recurrence with kv cache compression for efficient llm inference. *arXiv preprint arXiv:2402.09398*, 2024.
- [33] Piotr Nawrot, Adrian Łańcucki, Marcin Chochowski, David Tarjan, and Edoardo M Ponti. Dynamic memory compression: Retrofitting llms for accelerated inference. *arXiv preprint arXiv:2403.09636*, 2024.

- [34] Alexey Dosovitskiy, Lucas Beyer, Alexander Kolesnikov, Dirk Weissenborn, Xiaohua Zhai, Thomas Unterthiner, Mostafa Dehghani, Matthias Minderer, Georg Heigold, Sylvain Gelly, Jakob Uszkoreit, and Neil Houlsby. An image is worth 16x16 words: Transformers for image recognition at scale. In *ICLR*. OpenReview.net, 2021.
- [35] Daniel Bolya, Cheng-Yang Fu, Xiaoliang Dai, Peizhao Zhang, Christoph Feichtenhofer, and Judy Hoffman. Token merging: Your vit but faster. *arXiv preprint arXiv:2210.09461*, 2022.
- [36] Dachuan Shi, Chaofan Tao, Anyi Rao, Zhendong Yang, Chun Yuan, and Jiaqi Wang. Crossget: Cross-guided ensemble of tokens for accelerating vision-language transformers. *arXiv preprint arXiv:2305.17455*, 2023.
- [37] Siyuan Wei, Tianzhu Ye, Shen Zhang, Yao Tang, and Jiajun Liang. Joint token pruning and squeezing towards more aggressive compression of vision transformers. In *Proceedings of the IEEE/CVF Conference on Computer Vision and Pattern Recognition*, pages 2092–2101, 2023.
- [38] Yu Zhang, Yepeng Liu, Duoqian Miao, Qi Zhang, Yiwei Shi, and Liang Hu. Mg-vit: A multi-granularity method for compact and efficient vision transformers. *Advances in Neural Information Processing Systems*, 36, 2024.
- [39] Xinjian Wu, Fanhu Zeng, Xiudong Wang, Yunhe Wang, and Xinghao Chen. Ppt: Token pruning and pooling for efficient vision transformers. *arXiv preprint arXiv:2310.01812*, 2023.
- [40] Myle Ott, Sergey Edunov, Alexei Baevski, Angela Fan, Sam Gross, Nathan Ng, David Grangier, and Michael Auli. fairseq: A fast, extensible toolkit for sequence modeling. *arXiv preprint arXiv:1904.01038*, 2019.
- [41] Thomas Wolf, Lysandre Debut, Victor Sanh, Julien Chaumond, Clement Delangue, Anthony Moi, Pierric Cistac, Tim Rault, Rémi Louf, Morgan Funtowicz, et al. Transformers: State-of-the-art natural language processing. In *Proceedings of the 2020 conference on empirical methods in natural language processing: system demonstrations*, pages 38–45, 2020.
- [42] Zhiyuan Dang, Cheng Deng, Xu Yang, Kun Wei, and Heng Huang. Nearest neighbor matching for deep clustering. In *Proceedings of the IEEE/CVF conference on computer vision and pattern recognition*, pages 13693–13702, 2021.
- [43] J. Stuart Hunter. The exponentially weighted moving average. *Journal of Quality Technology*, 18:203–210, 1986. URL <https://api.semanticscholar.org/CorpusID:124743553>.
- [44] Dan Busbridge, Jason Ramapuram, Pierre Ablin, Tatiana Likhomanenko, Eeshan Gunesh Dhekane, Xavier Suau Cuadros, and Russell Webb. How to scale your EMA. In *NeurIPS*, 2023.
- [45] Petar Veličković, Guillem Cucurull, Arantxa Casanova, Adriana Romero, Pietro Lio, and Yoshua Bengio. Graph attention networks. *arXiv preprint arXiv:1710.10903*, 2017.
- [46] Ebtesam Almazrouei, Hamza Alobeidli, Abdulaziz Alshamsi, Alessandro Cappelli, Ruxandra Cojocaru, Mérouane Debbah, Étienne Goffinet, Daniel Hesslow, Julien Launay, Quentin Malartic, et al. The falcon series of open language models. *arXiv preprint arXiv:2311.16867*, 2023.
- [47] Noam Shazeer. Fast transformer decoding: One write-head is all you need. *arXiv preprint arXiv:1911.02150*, 2019.
- [48] Joshua Ainslie, James Lee-Thorp, Michiel de Jong, Yury Zemlyanskiy, Federico Lebrón, and Sumit Sanghai. Gqa: Training generalized multi-query transformer models from multi-head checkpoints. *arXiv preprint arXiv:2305.13245*, 2023.
- [49] Thomas Wolf, Lysandre Debut, Victor Sanh, Julien Chaumond, Clement Delangue, Anthony Moi, Pierric Cistac, Tim Rault, Rémi Louf, Morgan Funtowicz, et al. Huggingface’s transformers: State-of-the-art natural language processing. *arXiv preprint arXiv:1910.03771*, 2019.
- [50] Siva Reddy, Danqi Chen, and Christopher D. Manning. Coqa: A conversational question answering challenge. *Trans. Assoc. Comput. Linguistics*, 7:249–266, 2019.

- [51] Stephanie Lin, Jacob Hilton, and Owain Evans. Truthfulqa: Measuring how models mimic human falsehoods. In *ACL (1)*, pages 3214–3252. Association for Computational Linguistics, 2022.
- [52] Karl Cobbe, Vineet Kosaraju, Mohammad Bavarian, Mark Chen, Heewoo Jun, Lukasz Kaiser, Matthias Plappert, Jerry Tworek, Jacob Hilton, Reiichiro Nakano, et al. Training verifiers to solve math word problems. *arXiv preprint arXiv:2110.14168*, 2021.
- [53] Eleftheria Briakou, Colin Cherry, and George Foster. Searching for needles in a haystack: On the role of incidental bilingualism in palm’s translation capability. *arXiv preprint arXiv:2305.10266*, 2023.
- [54] Chaofan Tao, Lu Hou, Wei Zhang, Lifeng Shang, Xin Jiang, Qun Liu, Ping Luo, and Ngai Wong. Compression of generative pre-trained language models via quantization. In *Annual Meeting of the Association for Computational Linguistics*, 2022. URL <https://api.semanticscholar.org/CorpusID:247593909>.
- [55] Dachuan Shi, Chaofan Tao, Ying Jin, Zhendong Yang, Chun Yuan, and Jiaqi Wang. Upop: Unified and progressive pruning for compressing vision-language transformers. In *International Conference on Machine Learning*, pages 31292–31311. PMLR, 2023.
- [56] Chaofan Tao, Lu Hou, Haoli Bai, Jiansheng Wei, Xin Jiang, Qun Liu, Ping Luo, and Ngai Wong. Structured pruning for efficient generative pre-trained language models. In *Findings of the Association for Computational Linguistics: ACL 2023*, pages 10880–10895, 2023.
- [57] Zhongwei Wan, Che Liu, Mi Zhang, Jie Fu, Benyou Wang, Sibio Cheng, Lei Ma, César Quilodrán-Casas, and Rossella Arcucci. Med-unic: Unifying cross-lingual medical vision-language pre-training by diminishing bias. *Advances in Neural Information Processing Systems*, 36, 2024.
- [58] Zhongwei Wan, Che Liu, Xin Wang, Chaofan Tao, Hui Shen, Zhenwu Peng, Jie Fu, Rossella Arcucci, Huaxiu Yao, and Mi Zhang. Electrocardiogram instruction tuning for report generation. *arXiv preprint arXiv:2403.04945*, 2024.
- [59] Zhongwei Wan, Yichun Yin, Wei Zhang, Jiaxin Shi, Lifeng Shang, Guangyong Chen, Xin Jiang, and Qun Liu. G-map: general memory-augmented pre-trained language model for domain tasks. *arXiv preprint arXiv:2212.03613*, 2022.
- [60] Che Liu, Zhongwei Wan, Sibio Cheng, Mi Zhang, and Rossella Arcucci. Etp: Learning transferable ecg representations via ecg-text pre-training. In *ICASSP 2024-2024 IEEE International Conference on Acoustics, Speech and Signal Processing (ICASSP)*, pages 8230–8234. IEEE, 2024.
- [61] Che Liu, Zhongwei Wan, Yuqi Wang, Hui Shen, Haozhe Wang, Kangyu Zheng, Mi Zhang, and Rossella Arcucci. Benchmarking and boosting radiology report generation for 3d high-resolution medical images. *arXiv e-prints*, pages arXiv–2406, 2024.
- [62] Che Liu, Zhongwei Wan, Cheng Ouyang, Anand Shah, Wenjia Bai, and Rossella Arcucci. Zero-shot ecg classification with multimodal learning and test-time clinical knowledge enhancement. *arXiv preprint arXiv:2403.06659*, 2024.
- [63] Kangyu Zheng, Yingzhou Lu, Zaixi Zhang, Zhongwei Wan, Yao Ma, Marinka Zitnik, and Tianfan Fu. Structure-based drug design benchmark: Do 3d methods really dominate? *arXiv e-prints*, pages arXiv–2406, 2024.
- [64] Jing Xiong, Zhongwei Wan, Xiping Hu, Min Yang, and Chengming Li. Self-consistent reasoning for solving math word problems. *arXiv preprint arXiv:2210.15373*, 2022.
- [65] Zhenyu Liang, Yunfan Li, and Zhongwei Wan. Large scale many-objective optimization driven by distributional adversarial networks. *arXiv preprint arXiv:2003.07013*, 2020.
- [66] Zhenyu Liang, Yunfan Li, and Zhongwei Wan. Many-objective estimation of distribution optimization algorithm based on wgan-gp. *arXiv preprint arXiv:2003.08295*, 2020.

- [67] Zhongwei Wan, Xin Liu, Benyou Wang, Jiezhong Qiu, Boyu Li, Ting Guo, Guangyong Chen, and Yang Wang. Spatio-temporal contrastive learning-enhanced gnn for session-based recommendation. *ACM Transactions on Information Systems*, 42(2):1–26, 2023.
- [68] Lianmin Zheng, Wei-Lin Chiang, Ying Sheng, Siyuan Zhuang, Zhanghao Wu, Yonghao Zhuang, Zi Lin, Zhuohan Li, Dacheng Li, Eric Xing, et al. Judging llm-as-a-judge with mt-bench and chatbot arena. *Advances in Neural Information Processing Systems*, 36, 2024.

## A Appendix / supplemental material

### A.1 Limitations

The limitations of our work lie in the fact that we have used the original architecture of the large language model (LLM) without expanding it with additional compression techniques [5, 6] such as quantization [54], pruning [55, 56] and other efficient attention mechanisms. In our future research, we plan to explore methods to achieve the most extreme level of compression.

### A.2 Broader Impact

This paper presents a new method for compressing the KV cache in large language models (LLMs), highlighting the extensive impact of our technology. By optimizing the KV cache, our technique not only enables the use of large language models on devices with limited resources, such as smartphones and laptops, but it also preserves the accuracy of LLM inferences. This dual functionality aids in the widespread applications such as healthcare [57–63], math [17, 64], optimization [65, 66] and recommendation [67], and development of large-language models by ensuring they can operate effectively in various technological environments. Nevertheless, it is crucial to avoid the improper application of this compression method, particularly at high compression ratios, as it may lead to reduced performance and adversely affect everyday functionality.

### A.3 More Setting Details

In all our experiments, we used model weights downloaded from Huggingface as follows: for all Llama architectures, the Llama-1-7B model employed the 'huggyllama/llama-7b'<sup>1</sup> checkpoint, Llama-2-7B used the 'meta-llama/Llama-2-7b-hf'<sup>2</sup> version, Llama-2-13B utilized 'meta-llama/Llama-2-13b-hf'<sup>3</sup>, and for the latest Llama-3-8B, we used 'meta-llama/Meta-Llama-3-8B'<sup>4</sup>. In the Mistral architecture, the 'mistralai/Mistral-7B-Instruct-v0.2'<sup>5</sup> checkpoint was employed. For the Falcon architecture, 'tiiuae/falcon-7b'<sup>6</sup> was used. Additionally, for the evaluation metrics of the various sub-tasks such as "narrativeqa," "qasper," "multifieldqa\_en," and "hotpotqa" within the LongBench benchmark, please refer to the official benchmark repository<sup>7</sup>.

### A.4 Generated Samples of Multi-turn Conversations

To validate our D<sub>2</sub>O method's ability to preserve critical context information and generate correct and fluent responses in multi-turn dialogues, we employed the MT-bench dataset [68]. This dataset consists of 3.3K expert-level pairwise human preferences for responses generated by six models, including GPT-4 and LLaMA-13B, in response to 80 multi-turn questions. It is specifically designed to assess the performance of language models in producing contextually appropriate conversations. To ensure a fair experimental comparison, we followed the settings [13, 12] of using a KV cache budget of 2048 tokens. For D<sub>2</sub>O and H<sub>2</sub>O, we set the quantity of the top  $N$  important tokens at 48 and recent tokens  $M$  at 2000.

<sup>1</sup><https://huggingface.co/huggyllama/llama-7b>

<sup>2</sup><https://huggingface.co/meta-llama/Llama-2-7b-hf>

<sup>3</sup><https://huggingface.co/meta-llama/Llama-2-13b-hf>

<sup>4</sup><https://huggingface.co/meta-llama/Meta-Llama-3-8B>

<sup>5</sup><https://huggingface.co/mistralai/Mistral-7B-Instruct-v0.2>

<sup>6</sup><https://huggingface.co/tiiuae/falcon-7b>

<sup>7</sup><https://github.com/THUDM/LongBench>



especially when the retrieval task reaches a maximum length of 100k. In contrast, our D<sub>2</sub>O method, which employs a dynamic token merging strategy, effectively preserves the information of evicted tokens and mitigates the impact of KV cache compression on long-context retrieval.

### A.6 Inference Cost Analysis

To better understand the time overhead associated with prompt encoding and token generation after implementing token-level discriminative operations, we compared the time costs of prompt encoding to the total inference time. Our results, as illustrated in Table 8, show that the prompt encoding process, which utilizes token eviction and dynamic token merging operations, constitutes only a small fraction of the total time. Moreover, as the length of generation tokens increases, this proportion continues to decrease to 0.224%, indicating that the token merging operation is both efficient and less time-consuming.

Table 8: Inference time cost analysis of Llama 3-8B. The overall generation duration is calculated from the beginning of the decoding process to the conclusion of the generation sequence. Prompt encoding time spans from the initial prompt input to the completion of token eviction and dynamic token merging by D<sub>2</sub>O. The KV cache budget is established at 256 tokens with a ratio of  $M : N$  set at 1:3.

Prompt Len + Decoding Len	Overall Generation Duration (s)	Prompt Encoding Duration (s)	Decoding Time Per Token (s)	Prompt Encoding/Overall (%)
256+512	29.454	0.235	0.057	0.798%
512+1024	58.528	0.246	0.057	0.420%
1024+2048	121.191	0.328	0.059	0.271%
2048+4096	232.398	0.520	0.057	0.224%

### A.7 Extended Analysis of LongBench Experiment

This experiment mainly validate the capability of our D<sub>2</sub>O to handle longer text data under a low KV cache budget, we selected several representative tasks from the LongBench, including single-document QA (e.g., MultifieldQA), multi-document QA (such as HotpotQA and 2wikimQA), summarization (GovReport, TREC, and SAMSum), and code completion (Lcc RB-P). We specifically chose datasets exceeding 8k in length and only retained 20% KV cache budget. As shown in Table 9, D<sub>2</sub>O still demonstrates significant advantages even on datasets larger than 8k. Specifically, within the Llama-2-7B architecture, D<sub>2</sub>O outperforms the best baseline by 5.94 and 7.23 points in two summarization tasks, GovReport and TREC, respectively. This robustly validates the effectiveness of D<sub>2</sub>O’s dynamic layer and token-level strategies, which effectively compress extended textual information under a low KV cache budget.

Table 9: Performance evaluation of D<sub>2</sub>O across various models using a range of benchmarks from LongBench at 8k settings.

Model		MultifieldQA	HotpotQA	2wikimQA	GovReport	TREC	SAMSum	Lcc	RB-P
Llama-2-7B	Full Model	15.97	8.83	6.97	12.15	61.00	42.93	66.4	53.34
	Local Window	0.00	0.17	0.00	0.38	0.00	0.00	4.70	4.69
	StreamingLLM	15.05	6.68	5.77	6.72	52.67	41.39	62.17	46.82
	H <sub>2</sub> O	15.06	8.53	7.00	7.31	52.67	42.44	61.66	50.70
	RoCo	12.56	6.23	6.65	5.58	48.80	40.78	61.55	49.54
	D <sub>2</sub> O	15.66	9.10	8.04	13.25	59.00	44.23	65.36	53.34
	↑	0.61	0.57	1.04	5.94	7.23	1.79	3.70	2.64
Llama-3-8B	Full Model	22.48	11.64	12.17	24.8	73.00	43.43	73.81	54.42
	Local Window	2.84	3.81	6.08	0.59	35.00	10.18	37.20	22.26
	StreamingLLM	12.93	9.25	8.70	19.20	67.00	39.40	71.99	52.08
	H <sub>2</sub> O	15.50	10.54	9.30	20.57	70.00	42.23	71.54	50.40
	RoCo	14.23	10.11	8.88	18.56	66.89	40.12	69.98	51.12
	D <sub>2</sub> O	17.82	11.58	9.72	21.99	71.00	43.71	73.05	53.67
	↑	2.32	1.04	0.42	1.42	1.00	1.48	1.06	1.59

### A.8 Visualization of Attention Weights Across Various Datasets

In this section, we visualize the attention weight results of the prompts across various layers of models such as Llama-1-7B and Llama-3-8B on reasoning datasets like GSM8K [52] and COQA [50].



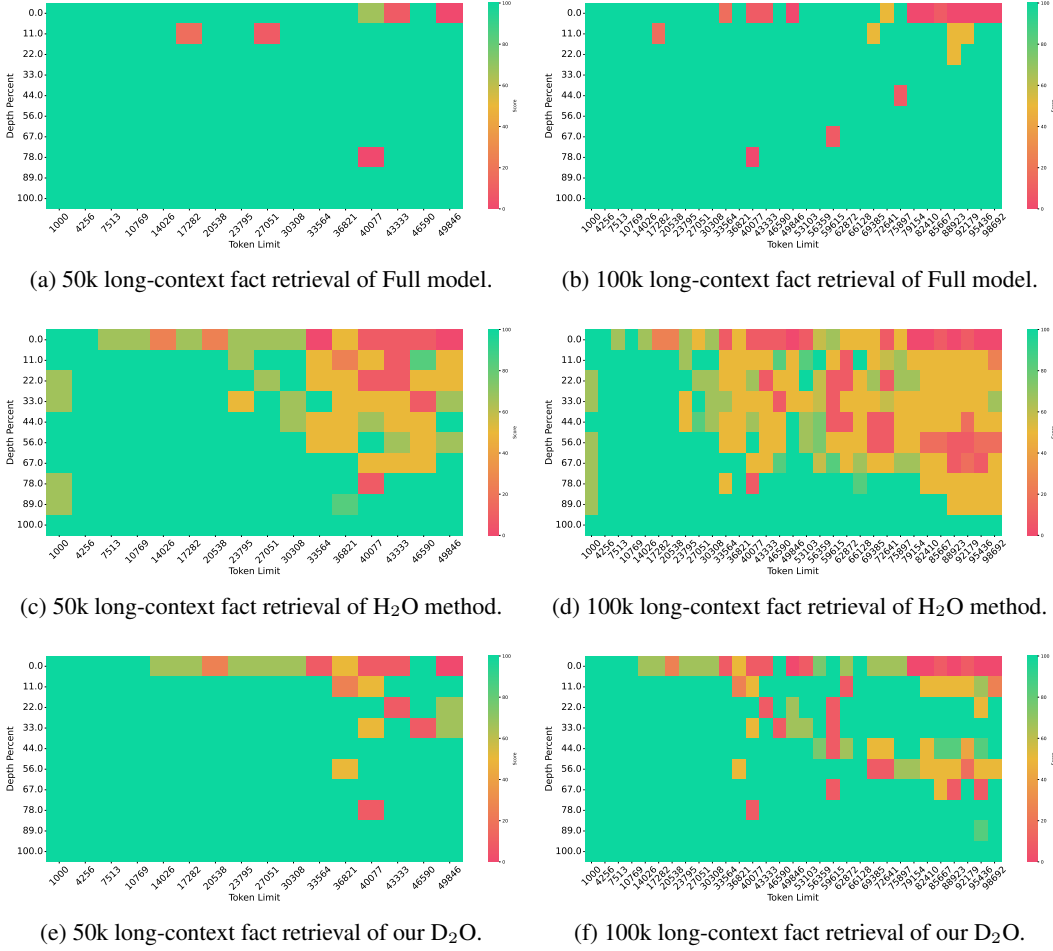
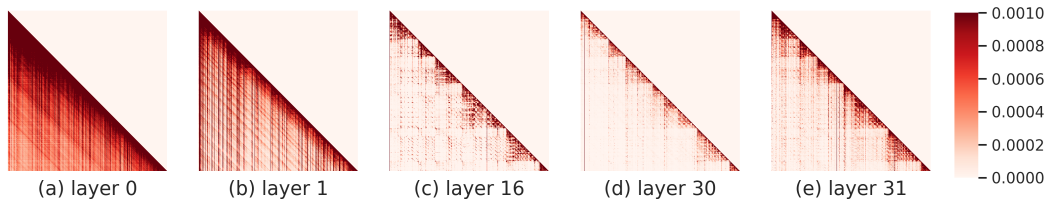
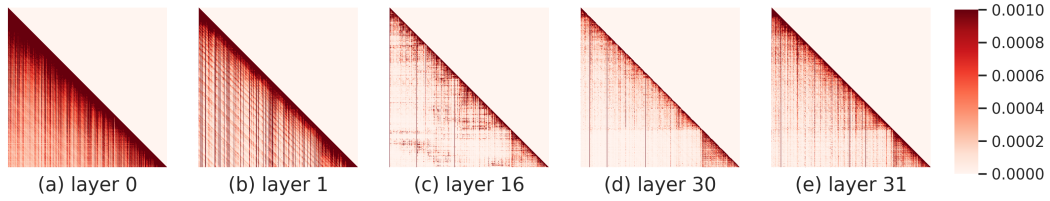


Figure 8: Visualization comparisons of long-context fact retrieval tasks for several methods.

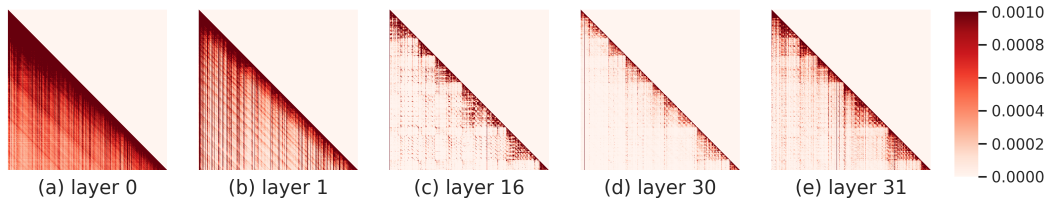
Consistent with the observations noted in Section 1 of the main text, a similar pattern exists across different models and datasets, wherein the lower layers of the models exhibit a higher density than the higher layers. Thus, this strongly corroborates our motivation for the layer-level discriminative operation, which employs different eviction ratio strategies for layers with varying densities of attention weights.



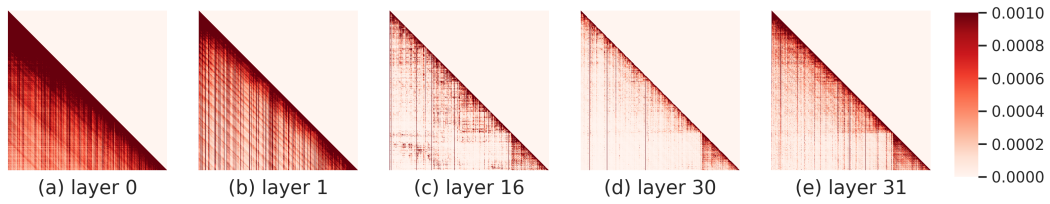
(a) Attention weight visualization for Llama-1-7b on GSM8K dataset.



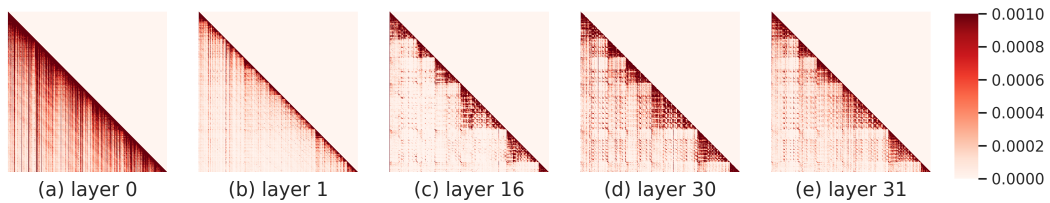
(b) Attention weight visualization for Llama-1-7b on COQA dataset.



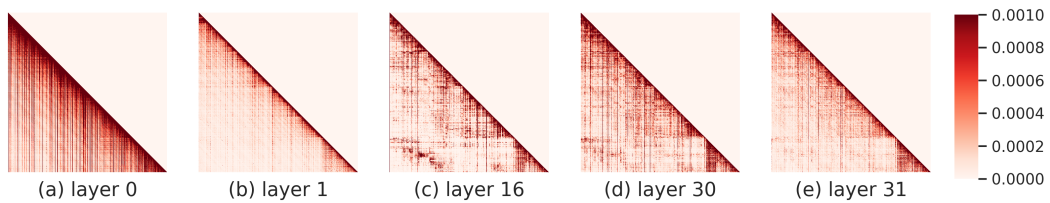
(c) Attention weight visualization for Llama-2-7b on GSM8K dataset.



(d) Attention weight visualization for Llama-2-7b on COQA dataset.



(e) Attention weight visualization for Llama-3-8B on GSM8K dataset.



(f) Attention weight visualization for Llama-3-8B on COQA dataset.

Figure 9: Attention weight visualization.